

# Localized States in Anthrylpolyenes: Influence of Geometry

---

**B. Heine and E. Sigmund**

Institut für Theoretische Physik, University of Stuttgart, Pfaffenwaldring 57, D-7000 Stuttgart 80, FRG

**S. Maier, H. Port and H. C. Wolf**

3. Physikalisches Institut, University of Stuttgart, Pfaffenwaldring 57, D-7000 Stuttgart 80, FRG

**F. Effenberger and H. Schlosser**

Institut für Organische Chemie, University of Stuttgart, Pfaffenwaldring 55, D-7000 Stuttgart 80, FRG

---

Combining group theoretical arguments and (extended) Hückel calculations, it is shown that terminally anthryl-substituted polyenes exhibit states almost completely localized at the substituents. These localized states are related to characteristic optical transitions in anthracene which also are observed in anthrylpolyenes independent of the length of the polyene chain.

*Keywords:* Electronic structure of large molecules; localization of electronic states

## INTRODUCTION

Molecules capable of storing and transferring information have achieved great interest in recent years.<sup>1-11</sup> In this paper we report model calculations on conjugated polyenes terminally substituted with anthracene showing the existence of localized states on the end-groups. These calculations were initiated by experimental studies on a variety of all-*trans*-polyenes with different substituents.<sup>1,2</sup> For anthrylpolyenes, characteristic changes in the absorption spectra depending on the substitution position of the anthracene have been observed. Further experimental details are presented and related to theory. In the next section the electronic states and their localization behaviour for the anthracene molecule are considered. We calculate the energy and eigenstates of the system in the Hückel approximation and show that from a group theoretical point of view this

treatment is sufficient for a qualitative description of the observed phenomena. Then the whole molecule is calculated in the Hückel approximation and the localization behaviour of the eigenfunctions for different coupling points of the chain to the anthracene is discussed. The two subsequent sections summarize the results of an extended Hückel calculation and show the influence of the geometry on energy and eigenvectors of the molecule. A closer inspection using a more involved MNDO calculation shows that the geometry of the molecule under investigation is already predicted correctly within the framework of extended Hückel calculations, thus allowing us to restrict ourselves in the present context to this easier and more transparent approach. In the Experimental and Results sections absorption spectra of anthrylpolyene with variable length of the polyene chain are discussed with respect to the theory.

## THE ELECTRONIC SPECTRA

Electronic spectra of anthracene and other polyacenes calculated in the PPP approximation give good agreement with optical experiments.<sup>12,13</sup> As a result of these calculations, the first  $\pi \rightarrow \pi^*$  transition of anthracene turns out to transform like  $B_{2u}$  and the next one like  $B_{3u}$ .

The reduction of the reducible 14-dimensional representation  $\Gamma$  of the symmetry group  $D_{2h}$  consisting of the 14  $p_z$  orbitals  $\phi$  of anthracene (Fig. 1) yields

$$\Gamma = 3A_{1u} + 4B_{1u} + 3B_{2g} + 4B_{3g} \quad (1)$$

leading to a reduction of the 14-dimensional eigenvalue problem to only 3- and 4-dimensional ones.

The basis functions of the  $A_{1u}$  and  $B_{2g}$  representations are given by

$$\Psi_{A_{1u}}^1 = \frac{1}{2}(\phi_{10a} - \phi_{8a} + \phi_{9a} - \phi_{4a}) \quad (2)$$

$$\Psi_{A_{1u}}^2 = \frac{1}{2}(\phi_5 - \phi_8 + \phi_1 - \phi_4) \quad (3)$$

$$\Psi_{A_{1u}}^3 = \frac{1}{2}(\phi_6 - \phi_7 + \phi_2 - \phi_3) \quad (4)$$

$$\Psi_{B_{2g}}^1 = \frac{1}{2}(\phi_{10a} + \phi_{8a} - \phi_{9a} - \phi_{4a}) \quad (5)$$

$$\Psi_{B_{2g}}^2 = \frac{1}{2}(\phi_5 + \phi_8 - \phi_1 - \phi_4) \quad (6)$$

$$\Psi_{B_{2g}}^3 = \frac{1}{2}(\phi_6 + \phi_7 - \phi_2 - \phi_3) \quad (7)$$

None of them has contributions of wavefunctions at atom 9 or 10.

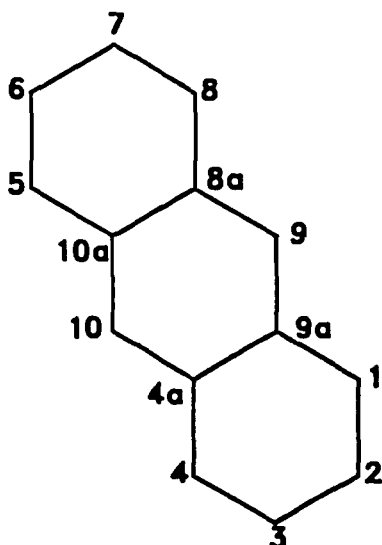


Figure 1. Anthracene. The atoms are numbered according to the notation commonly used in chemistry (IUPAC).

Depending on the choice of the Hamiltonian describing the system, we obtain for the eigenfunctions with  $A_{1u}$  and  $B_{2g}$  symmetry different linear combinations of the above basis functions, the amplitudes of which are all equal to zero at the atoms 9 and 10. This result is independent of the special form of the Hamiltonian and not only valid for the Hückel and extended Hückel approximation chosen in this paper.

To illustrate this statement and to investigate its consequences on the behaviour of the eigenfunctions of anthrylpolyenes, we perform a Hückel approximation with the Hamiltonian

$$H = \sum_n (t_{n,n+1} |\Phi_{n+1}\rangle \langle \Phi_n| + \text{h.c.}) \quad (8)$$

and the transfer integrals

$$t_{n,n+1} = - \langle \Phi_n | H | \Phi_{n+1} \rangle \quad (9)$$

In the case of the anthracene molecule,  $t_{n,n+1}$  is assumed to be constant and equal to  $\beta_a$  and we obtain the electronic spectra shown in Fig. 2.

When we couple a polyene chain to the anthracene, we would expect that an orbital having a node at the coupling point will remain unchanged and still be localized on the end-groups.

In Fig. 3, the wavefunctions of the first unoccupied orbitals of anthracene and of the corresponding orbitals of a dianthrylpolyene, calculated in the Hückel approximation [using the Hamiltonian (8)] are shown.

For the transfer integrals in the polyene chain, we adopted values given in the literature,<sup>14</sup>  $\beta_d = -3.35$  eV and  $\beta_s = -2.65$  eV, for the double

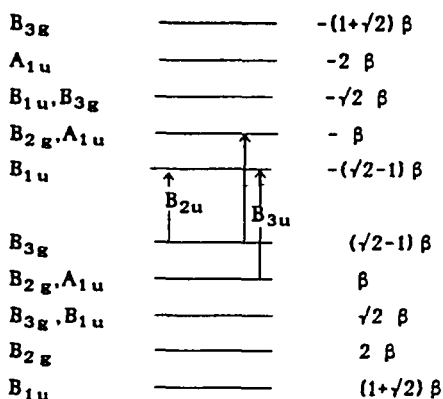


Figure 2. Energy spectra of anthracene, calculated in the Hückel approximation.

and single bonds, respectively. For the anthracene structure we chose  $\beta_a = -3.5$  eV. The first two values reproduce the gap of an infinite *trans*-(CH)<sub>x</sub> chain and the value  $\beta_a$  the first  $\pi \rightarrow \pi^*$  transition of anthracene.

Obviously an orbital having a node at the coupling point really remains localized on the anthracene whereas an orbital with finite amplitude at that point becomes delocalized over the whole molecule. Nevertheless this orbital also shows a strong similarity with the corresponding anthracene orbital, in particular the symmetry properties are the same as in anthracene. Hence the symmetry of the anthracene still influences strongly the wavefunctions of the dianthrylpolyene, and those dianthrylpolyene orbitals at least which are mainly localized on the anthracene can still be characterized by the symmetry behaviour of anthracene.

Additionally, in Fig. 3 it can be seen that this result does not depend on the nearest-neighbour interaction chosen in the Hückel calculation. Because the contributions of the adjacent atoms

have different signs, their interaction with the chain is neutralized and cannot lead to a change in the localization behaviour of the molecule.

The eigenenergy of an orbital remaining localized on the anthracene in the anthrylpolyene is the same as that of anthracene, whereas the energy of a delocalized orbital is changed. Table 1 shows the eigenenergies for a molecule with a chain of five double bonds between the two anthracene substituents. In the first column of data the energies of anthracene are given, in the second the energies of the whole molecule substituted in the 9-position, and in the third and fourth those of the 2- and 1-substituted molecules, respectively. For the substitution in the 9-position all the  $A_{1u}$  and  $B_{2g}$  orbitals remain unchanged owing to their nodes at the coupling points, whereas for the substitution in the 2- and 1-positions only one  $A_{1u}$  and one  $B_{2g}$  orbital remain unchanged (all these orbitals are now doubly degenerated caused by the two anthracene substituents).

These results do not depend on either the length of the chain between the end-groups or the choice

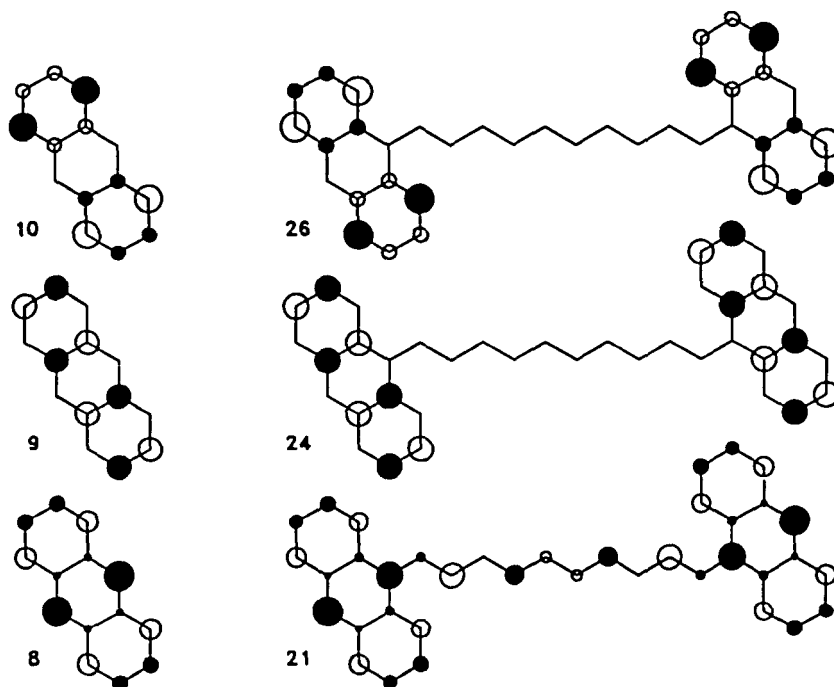


**Figure 3.** Eigenfunctions of anthracene, calculated in the Hückel approximation, and corresponding functions of a dianthrylpolyene. The black and white circles indicate negative and positive signs of the wavefunctions, respectively

Table 1. Eigenenergies (eV) for anthracene and three differently substituted anthrylpolyenes.

	Anthracene	9A-P <sub>5</sub> -9A	2A-P <sub>5</sub> -2A	1A-P <sub>5</sub> -1A
1 B <sub>1u</sub>	- 8.449749	- 8.554771	- 8.478356	- 8.505669
2 B <sub>2g</sub>	- 7.000000	- 8.554704	- 8.478333	- 8.505627
		- 7.000000	- 7.144196	- 7.135294
		- 6.999985	- 7.143093	- 7.134299
		- 5.898669	- 5.866009	- 5.827905
		- 5.672155	- 5.615208	- 5.491866
		- 5.333009	- 5.302343	- 5.205265
3 B <sub>1u</sub>	- 4.949751			
4 B <sub>3g</sub>	- 4.949748	- 4.949748	- 4.949749	- 4.949748
		- 4.949746	- 4.949748	- 4.949748
		- 4.748904	- 4.768595	- 4.809696
		- 3.895677	- 4.152771	- 4.252212
5 A <sub>1u</sub>	- 3.500001			
6 B <sub>2g</sub>	- 3.500001	- 3.500000	- 3.781365	- 3.811494
		- 3.500000	- 3.500000	- 3.500000
		- 3.500000	- 3.500000	- 3.500000
		- 3.499999	- 3.310070	- 3.318369
		- 2.902820	- 2.418864	- 2.523123
		- 1.973029	- 1.645896	- 1.767978
7 B <sub>3g</sub>	- 1.449750	- 1.293379	- 1.397805	- 1.356265
		- 0.8668033	- 1.053622	- 0.9696829
		0.8668025	1.053619	0.9696818
		1.293378	1.397803	1.356264
8 B <sub>1u</sub>	1.449748	1.973031	1.645894	1.767980
		2.902818	2.418860	2.523122
9 A <sub>1u</sub>	3.500000			
10 B <sub>2g</sub>	3.500003	3.500000	3.310067	3.318368
		3.500000	3.500000	3.499999
		3.500000	3.500001	3.500001
		3.500001	3.781360	3.811494
		3.895676	4.152770	4.252208
		4.748899	4.768594	4.809691
11 B <sub>1u</sub>	4.949751			
12 B <sub>3g</sub>	4.949747	4.949747	4.949749	4.949747
		4.949748	4.949749	4.949749
		5.333008	5.302336	5.205262
		5.672150	5.615202	5.491865
		5.898670	5.866005	5.827903
13 A <sub>1u</sub>	7.000002	7.000000	7.143100	7.134302
		7.000000	7.144203	7.135296
14 B <sub>3g</sub>	8.449747	8.554714	8.478337	8.505623
		8.554782	8.478360	8.505665

of the parameters  $\beta_d$ ,  $\beta_s$ , and  $\beta_a$ . For structures consisting of only one anthracene coupled to a polyene chain we obtained the same results with the only difference that in this case the localized orbitals are not degenerated.

With the help of symmetry we can also correlate our results with the absorption experiments reported under Experimental and Results. The absorption line under investigation corresponds to the anthracene transition which has the symmetry  $B_{3u}$  (see Fig. 2). If we took into account configuration interaction which would be necessary to obtain quantitative results, the degenerate  $B_{3u}$  transitions shown in Fig. 2 would split off and lead to one experimentally observable, allowed transition and one forbidden transition. This has been shown, for example, in reference 12. Both transitions, however, have the same localization behaviour and so will have, of course, any linear combination of them. With this argument we can relate the experimentally observed  $B_{3u}$  ( $S_3$ ) transition to the transitions drawn in Fig. 2 and can connect the existence of localized orbitals with the unchanged absorption line which has been observed experimentally.

So far the calculations have shown that the  $B_{3u}$  transitions in which we are interested involve one localized and one delocalized orbital. As will be shown in the next section with the help of more sophisticated calculations, actually both orbitals are localized because of the geometry of the molecule, which cannot be taken into account in the Hückel approximation.

### TOTAL ENERGY FOR NON-PLANAR MOLECULAR CONFORMATION

If we consider the molecular structure in more detail, taking into account the hydrogen atoms (Fig. 4), we expect steric hindrance caused by the hydrogen atoms (marked with arrows). To take such a steric hindrance into account the anthracenes were rotated around an axis defined by angles  $\phi$  and  $\theta$  (Fig. 4). This leads to a non-planar structure of the molecule which no longer allows a separation of the  $\pi$  and  $\sigma$  electron systems as assumed above and therefore the total energy of this configuration was calculated in the extended Hückel approximation. For this calculation we used a basis set<sup>15</sup> consisting of hydrogen Slater orbitals with exponent 1.0 and 2s and 2p carbon Slater orbitals with exponent 1.625. The diagonal matrix elements  $H_{ii}$  are chosen as valence state ionization potentials:

$$\begin{aligned} H_{ii}(C_{2p}) &= -11.4 \text{ eV} \\ H_{ii}(C_{2s}) &= -21.4 \text{ eV} \\ H_{ii}(H_{1s}) &= -13.6 \text{ eV} \end{aligned} \quad (10)$$

and the non-diagonal matrix elements  $H_{ij}$ :

$$H_{ij} = 0.5K(H_{ii} + H_{jj})S_{ij} \quad (11)$$

where  $K$  is taken to be 1.75.<sup>15</sup>

Varying the total energy as a function of the angles  $\phi$  and  $\theta$  we obtain a minimum of the energy for an angle  $\phi$  of about  $30^\circ$  and an angle  $\theta$  of  $90^\circ$ , which corresponds to rotation of the anthracene

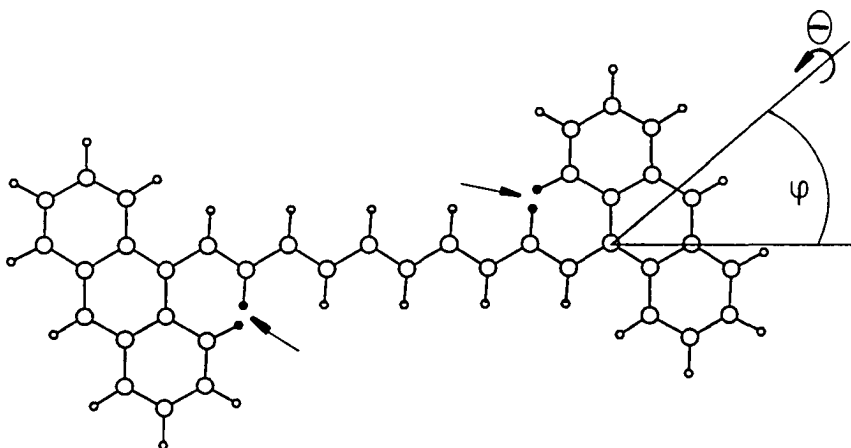


Figure 4. Structure showing the angle between the horizontal axis in the molecule plane and the rotation axis ( $\phi$ ) and the rotation angle around this axis ( $\theta$ ).

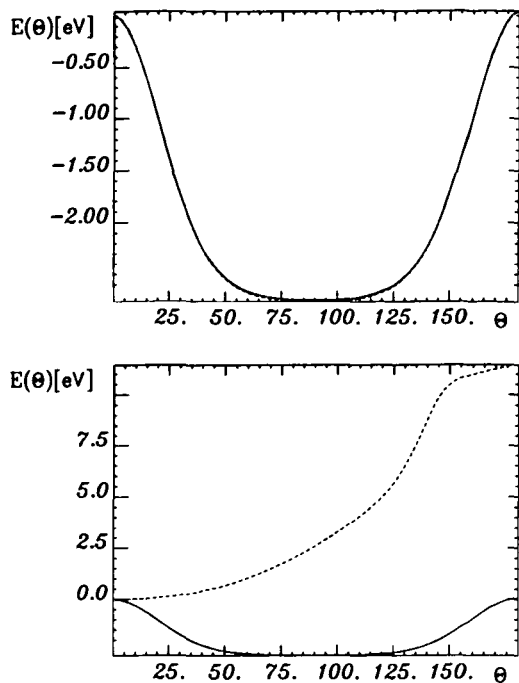


Figure 5. (a) Total energy of A-P<sub>5</sub>-CH<sub>3</sub> (—) and A-P<sub>9</sub>-CH<sub>3</sub> (---). (b) substitution in 9-position (—), 1-position (---) and 2-position (·····).

around the first C—C bond of the polyene chain. In Fig. 5a the change in the total energy as a function of the angle of rotation  $\theta$  around the first C—C bond is shown. The minimum energy is exactly at  $\theta = 90^\circ$ , but it is fairly flat, the difference between  $75^\circ$  and  $90^\circ$  being very small. Obviously already at  $\theta = 75^\circ$  the steric hindrance no longer exists and therefore further rotation cannot give a further gain in energy.

This effect is only caused by the anthracene end-group, and therefore we obtain identical results for different lengths of the polyene chain. This can also be seen in Fig. 5a, where we show the energy decrease for 9-anthrylpolyenes with five and nine double bonds. The absolute values of the total energy for these two molecules are, of course, different, but the change in the total energy we obtain by rotating the end-group around the first C—C bond is identical for both systems, however.

This behaviour occurs only for the molecule substituted in the 9-position, as will be shown below. Figure 5b shows the change in total energy of the molecule versus  $\theta$  at  $\phi = 30^\circ$  for the three different types of substitution. The zero point of

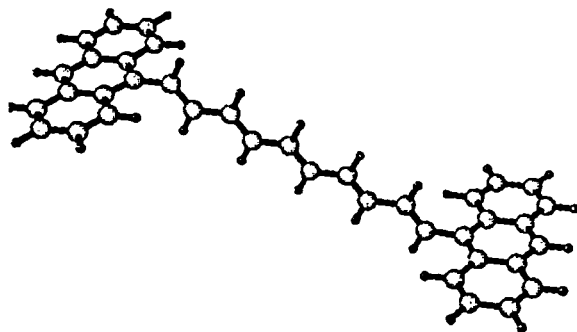


Figure 6. Geometry of the dianthrylpolyene, calculated with an MNDO procedure.

the energy scale in these graphs is chosen as the total energy of the planar molecules. There is a considerable decrease in energy only for the molecule substituted in the 9-position. For the other molecules there is no decrease in energy. As a result of these calculations, we conclude that the 9-anthrylpolyene cannot be a planar molecule independent of the chain length of the polyene, whereas the molecules substituted in the 1- or 2-position should be nearly planar.

Additionally we made a geometry optimization, using an MNDO<sup>16</sup> procedure and varying all coordinates. The resulting geometry is shown in Fig. 6. As already predicted with extended Hückel calculations, the whole molecule is non-planar because the anthracene plane is rotated with respect to the polyene plane. Hence it has been verified that the extended Hückel calculations give the correct geometry of the molecule. The rotation between the anthracene and polyene molecular planes influences the energy and localization behaviour of the wavefunctions of the whole molecule. This will be investigated in the next section.

### STERIC EFFECTS ON ENERGY SPECTRA AND WAVEFUNCTIONS

To describe the molecule within the framework of the extended Hückel approximation, we use a set of 66 basis functions consisting of 2s and 2p carbon orbitals and 1s hydrogen orbitals. The reduction of the 66-dimensional representation of anthracene yields

$$\Gamma = 14A_{1g} + 3A_{1u} + 12B_{1u} + 4B_{1u} + 3B_{2g} \\ + 14B_{2u} + 4B_{3g} + 12B_{3u}$$

Calculating the energy spectra, we obtain

$\pi$ 38	-6.861187	—	$B_{3g}$
$\pi$ 37	-7.096995	—	$B_{1u}$
$\pi$ 36	-8.286704	—	$A_{1u}$
$\pi$ 35	-8.350252	—	$B_{2g}$
$\pi$ 34	-9.736988	—	$B_{1u}$
		$\uparrow$	$B_{3u}$
		$\uparrow$	$B_{2u}$
$\pi$ 33	-11.77077	—	$B_{3g}$
$\sigma$ 32	-12.21957	—	$B_{1g}$
$\sigma$ 31	-12.55395	—	$A_{1g}$
$\pi$ 30	-12.57952	—	$B_{2g}$
$\pi$ 29	-12.79478	—	$A_{1u}$

and with the same arguments as under Electronic Spectra we can assign the  $B_{2u}$  and  $B_{3u}$  transition to

the transitions indicated by arrows. We note that, as expected, we obtain no mixing between  $\pi$  and  $\sigma$  orbitals and the  $\pi$  orbitals have wavefunctions identical with those of the Hückel approximation.

Considering the wavefunctions of the whole molecule, we obtain the same results as in the Hückel approximation: the  $A_{1u}$  (number 36 above) and  $B_{2g}$  (30) orbitals remain unchanged in energy and are totally localized on the end-groups for all three mentioned types of substitution. In Fig. 7a-c the wavefunctions corresponding to the  $A_{1u}$  (36) orbital in pure anthracene are shown. We see that we obtain exactly the same wavefunctions as for the pure anthracene (see Fig. 3, wavefunction number 9).

Let us consider what happens when the anthracenes are rotated around the last C—C bond. Of course, there is a mixing of  $\pi$  and  $\sigma$  orbitals, but the localized orbitals discussed above do not

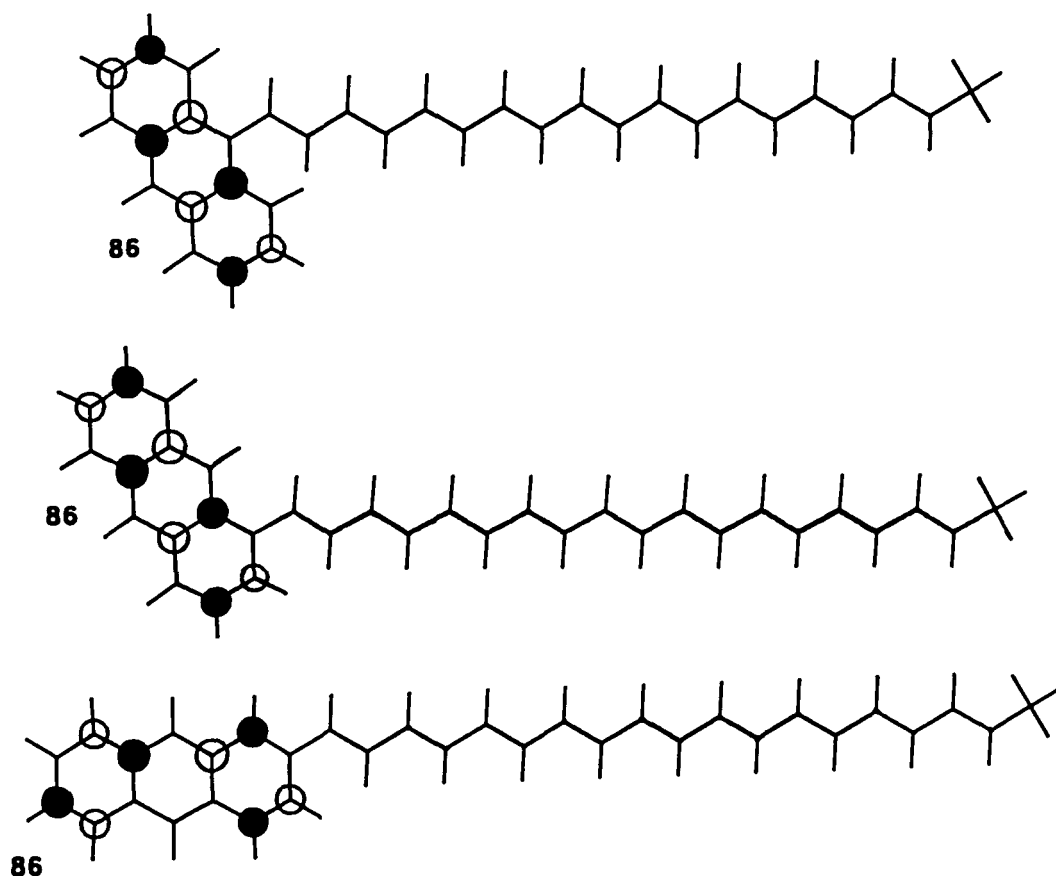


Figure 7. Wavefunctions for substitution in (a) the 9-, (b) the 1- and (c) the 2-position.

change their localization behaviour, but remain completely localized on the end-groups. In contrast, the delocalized orbitals change both energy and wavefunction considerably with increasing angle  $\theta$ . Calculating the eigenfunctions for the geometry shown in Fig. 6, we see that most of the orbitals have become now either anthracene or polyene orbitals and the delocalization of these orbitals has nearly disappeared. These results are obtained for chain lengths between 4 and 19 double bonds. Consequently, the  $B_{3n}$  transition under consideration is really a transition from an orbital localized predominantly on anthracene to another orbital with the same localization behaviour and corresponds in this approximation to a state localized predominantly on the end-group.

## EXPERIMENTAL

To investigate the influence of the molecular geometry and of the polyene chain length, a variety of anthryl-substituted all-*trans*-polyenes were selected, which can be represented by  $x\text{A}-\text{P}_m-x\text{A}$  and  $x\text{A}-\text{P}_n-\text{CHO}$ , where  $x$  = substitution position (1, 2 or 9, see Fig. 7) and  $m, n$  = number of conjugated double bonds,  $m = 5, 9$  and  $13$  and  $n = 4, 8$  and  $12$ .

Optical absorption spectra were recorded using a conventional SP8-250 spectrophotometer (Pye Unicam) with 0.5 nm resolution. The spectra were measured at room temperature in methylene chloride ( $\text{CH}_2\text{Cl}_2$ ) as solvent at concentrations between  $10^{-7}$  and  $10^{-5}$  mol l $^{-1}$ . In this range all results did not depend on concentration.

## RESULTS

The electronic absorption spectra of the anthryl-polyenes were systematically compared, taking those of the individual compounds, anthracenes and polyenes of variable length as references (Fig. 8a). The spectra of the substituted polyenes 9A-P $_n$ -9A (Fig. 8b) are composed essentially of the main absorption bands of end-groups and chain. The broad absorption bands between 600 and 400 nm show the dependence of chain length  $n$  that is characteristic of excited polyene states:<sup>17</sup> with increasing number of double bonds the polyene absorption shifts to lower energies and the molar extinction coefficient,  $\epsilon$ , increases. These absorption bands are assigned to polyene  $S_2$

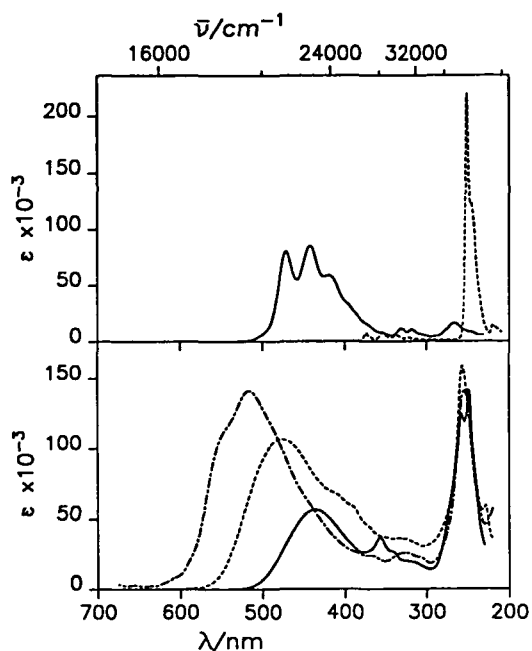


Figure 8. Absorption spectra of (a) polyene P $_n$  (—) and anthracene (A) (---) and (b) 9A-P $_n$ -9A with  $n = 5$  (—), 9 (---) and 13 (- · - ·).

absorption that dominates the spectra of unsubstituted polyenes.

Between 300 and 220 nm the spectra show a strong absorption band that hardly changes with increasing chain length of the polyene. This absorption also appears, with half the intensity, in unilaterally 9-anthryl-substituted polyenes.<sup>18</sup> Therefore, this band is assigned to the  $S_3$  absorption of the anthracene molecule.<sup>19</sup> Its integral intensity per 9-anthryl substituent is in the range 75–90% as compared with unsubstituted anthracene. This result does not depend on the number of conjugated double bonds in the polyene chain. Obviously in the anthrylpolyenes the anthracene substituents still exhibit localized ( $S_3$ ) electronic states which can be excited selectively. The integral intensity of this absorption band can be taken as a measure of the degree of localization.

The absorption spectra of 2A-P $_n$ -CHO shown in Fig. 9a reveal differences relative to the spectra of 9A-P $_n$ -CHO and 9A-P $_n$ -9A (see Fig. 8b): the integral absorption intensity round 250 nm is more strongly reduced, to 40% of the integral absorption intensity of  $S_3$  in unsubstituted anthracene.

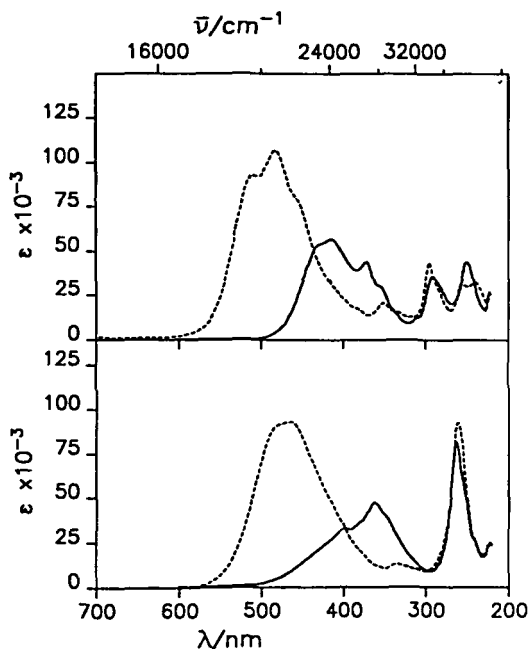


Figure 9. Absorption spectra of (a) 2A- $P_n$ -CHO with  $n = 4$  (—) and 8 (---) and (b) 1,4-DM-9A- $P_n$ -CHO with  $n = 4$  (—) and 8 (---).

Additionally, an absorption band at about 290 nm appears which cannot be found in the spectra of unsubstituted polyenes or anthracene and therefore must be assigned to an electronic state of the whole supermolecule 2A- $P_n$ -CHO.

The spectra of 1,4-DM-9A- $P_n$ -CHO (1,4-dimethylanthyryl-polyenes with substitution in the 9-position) (see Fig. 8b) exhibit the same spectral features as measured for 9A- $P_n$ -CHO or 9A- $P_n$ -9A. The DMA absorption bands are broadened compared with unsubstituted 1,4-DMA. The integral intensities of the anthryl absorption in 1,4-DM-9A- $P_n$ -CHO are not reduced with respect to unsubstituted 1,4-DMA.

In these experiments a sequence of relative anthracene absorptions has been found:  $I(\text{DM9A}) > I(9A) > I(2A)$ . These differences in the localization behaviour can be correlated with the effects of substitution position and steric hindrance considered in the theoretical section. The evaluation of experimental data on 1A- $P_m$ -1A ( $m = 1-6$ ), taken from the literature,<sup>20</sup> provides results that complement the sequence obtained. The estimation of the integral intensities of the anthryl  $S_3$  band in 1A- $P_m$ -1A gives values between 50 and

70% of the intensity of unsubstituted anthracene. With respect to its degree of localization, 1A-substitution lies between 9A- and 2A-substitution.

## CONCLUSIONS

For anthrylpolyenes with different chain lengths and geometries, the existence of electronic states localized predominantly on the end-groups has been proved theoretically. The corresponding energy levels are the same as in anthracene. Minimization of the ground-state energy with respect to rotation of the anthryl substituent around the last bond of the polyene chain predicts a non-planar configuration for the 9-anthrylpolyene whereas the anthrylpolyenes substituted in the 1- or 2-position are expected to be nearly planar. The out-of-plane rotation of the anthracene enhances the degree of localization of the non-localized energy levels and makes them more similar to the states in anthracene. Hence the theory provides an explanation for the experimentally observed anthryl- $S_3$ -absorption lines in anthrylpolyenes, which vary significantly in their relative intensities depending on the coupling position.

## Acknowledgements

The authors are grateful to D. Baeriswyl and M. Wagner for fruitful discussion and to the Deutsche Forschungsgemeinschaft for financial support.

## REFERENCES

1. F. Effenberger, H. Schlosser, P. Bauerle, St. Maier, H. Port and H. C. Wolf, *Angew. Chem.* **100**, 274 (1988).
2. St. Maier, H. Port, H. C. Wolf, F. Effenberger and H. Schlosser, *Synth. Met.* in press (1988).
3. R. W. Munn, *Chem. Ber.* **20**, 518 (1984).
4. T. S. Arrhenius, M. Blanchard-Desce, M. Dvolaitzky, J. M. Lehn and J. Malthete, *Proc. Natl. Acad. Sci. USA* **83**, 5355 (1986).
5. J. M. Lehn, *Angew. Chem., Int. Ed. Engl.* **27**, 89 (1988).
6. A. Leitner, M. E. Lippisch, S. Draxler, M. Riegler and F. R. Aussenegg, *Thin Solid Films* **132**, 55 (1982).
7. J. R. Miller, L. T. Calcaterra and G. L. Gloss, *J. Am. Chem. Soc.* **106**, 3047 (1984).
8. H. Heule and M. E. Michel-Beyerle, *J. Am. Chem. Soc.* **107**, 8286 (1985).
9. J. A. Schmidt, A. Siemearczuk, A. C. Weedon and J. R. Bolton, *J. Am. Chem. Soc.* **107**, 6112 (1985).
10. D. Gust, T. A. Moore, P. A. Lidell, G. A. Nemeth, L. R. Makings, A. L. Moore, D. Barret, P. J. Pessiki, R. V.

- Bensasson, M. Rougee, C. Cachaty, F. C. Schryver, M. Van der Auweraer, A. R. Holzwarth and J. S. Connolly, *J. Am. Chem. Soc.* **109**, 846 (1987).
11. D. N. Beratan, *J. Am. Chem. Soc.* **108**, 4321 (1986).
  12. P. Pariser, *J. Chem. Phys.* **24**, 250 (1956).
  13. W. Mofitt, *J. Chem. Phys.* **22**, 320 (1954).
  14. P. R. Surjan and H. Kuzmany, *Phys. Rev. B* **33**, 2615 (1986).
  15. R. Hoffmann, *J. Chem. Phys.* **39**, 1397 (1963).
  16. M. J. S. Dewar and W. Thiel, *J. Am. Chem. Soc.* **99**, 4899, 4907 (1977).
  17. B. S. Hudson, B. E. Kohler and K. Schulten, in *Excited States VI*, edited by E. C. Lim. Academic Press, New York (1982).
  18. St. Maier, Dissertation, Universität Stuttgart (1988).
  19. J. B. Birks, *Organic Molecular Photophysics*, Vol. 1. Wiley, London (1973).
  20. K. Mandal and T. N. Misra, *Bull. Chem. Soc. Jpn.* **49**, 198 (1976).